Stability and Antimicrobial Activity of Transition Metal (II) Complexes with SNO and ONO Functionalized Ligand: A Computational Study

Fakhr M. Abu-Awwad[1*] and Nabil M. El-Halabi[1]

[1]*Gaza- Chemistry Department, Islamic University of Gaza, Post Box 108, Palestine.*

Authors' contributions

This work was carried out in equal collaboration between both authors. Author NMEH designed the experimental part and concluded his results and then wrote the first draft of his findings. Author FMAA performed the computational investigations along with its subsequent analysis and wrote his part of the manuscript. Both authors managed the analyses of the study, confirm the findings, read and approved the final manuscript.

Original Research Article

ABSTRACT

In this work, the structural, surface potential, and antimicrobial aspects of a set of recently synthesized and published complexes of five transition metals(II) are investigated using the semiempirical PM6 and B3LYP/6-31G* methods. The complexes ML_2 [M = Ni, Cu, and Zn] are mainly composed of 2-thiophenecarbaldehyde isonicotinoyl hydrazone containing a trifunctional SNO-donor system. Experimentally, the complexes were synthesized and characterized using their conductivity, IR, and partially using ^{1}H NMR, and MS spectra, where they show similar properties to those in their analogous NNO functionalized ligand and ONO donor ligand. The attained wavefunction for each of the complexes was subsequently used to compute six molecular descriptors which were then investigated in light of their reported antimicrobial activities against *Escherichia coli, Staphylococcus aureus*, and *Pseudomonas aeruginosa*. The findings are further explored to elucidate the impact of the structural features on the complex biological activity. It is concluded that the type of transition metal is significantly impacting the antimicrobial activity of the complex, where the structural features of Mn(II) counterpart complexes were computationally inspected and their untested biological activities was predicted.

Corresponding author: Email: fakhr@iugaza.edu.ps;

1. INTRODUCTION

Transition metal (TM) complexes of hydrazones have been used for research in various applications of biological chemistry. Similarly, metal complexes of S-, N-, and O- chelating ligands have been attracting researchers due to their interesting structural features as chelating agents associated with their remarkable physicochemical properties, pronounced biological activities and their use as models for metalloenzyme active sites [1-3].

Schiff-bases have been widely used as ligands in the field of coordination chemistry, where they show a strong tendency to coordinate through the azomethine N with various metals and hence to stabilize them into upgraded oxidation states. As an example, complexes of tridentate Schiff-bases show a great range of catalytic, biological, antifungal, antitumor, and anti-HIV activities [4].

In the last few decades, extensive experimental and computational research has been aiming at developing new antimicrobial agents. Several factors including a heavy antibiotic worldwide use and person-to-person spread of bacteria have significantly increased the antibiotic-resistance through genetic mutation [5]. Unfortunately, while very few new antibiotics are in advanced development, very few new antibacterial drugs with a completely novel mechanism of action have been approved since 2006. This situation pushed researchers to discuss if humanity reached the Post-Antibiotic era [6].

Along this line in the last few years, while we were contributing by synthesizing a set of transition metal(II) complexes with SNO functionalized ligands, two research articles have been published with almost the same experimental content we planned for [3,7]. Therefore, we are interested here in further computationally examining these complexes and other analogous complexes with ONO and SNO functionalized ligands for their thermodynamic stabilities and biological activities associated with various structural modifications.

Computational approaches such as electronic calculations, genomics, molecular simulation and dynamics, molecular docking, structural/functional class prediction, and quantitative structure–activity relationships (QSARs) have been advantageous in antimicrobial drug discovery and design. They have become standard tools in the quest to develop novel anti-inflammatory pharmaceutical products through providing a rational basis for the selection of chemical structure [8-10]. The majority of QSAR described in the literature deals with the different classes of organic substances while very few studies cover QSAR analyses of inorganic, organometallic, or coordination compounds, because of the lack of a suitable tool for calculating descriptors for heavy atoms [11].

The recently implemented semiempirical method in Wavefunction SPARTAN '10, PM6 was designed primarily for the investigation of molecular species of biochemical interest [12,13]. The method is a major semiempirical method available in the package that may be applied to transition metals. It successfully reproduces the heats of formation and geometries of small molecules, simple organic and inorganic crystals, and a hormone with good accuracy [14]. However, it is common that calculations including metal complexes are challenging where the systems often involve multiple open shells with high and low spin complexes while the Jahn-Teller effect should be taken in consideration and the calculated systems should distort so as to lower the symmetry.

In this work, we combine experimental tools employed to synthesis and characterize our targeted structures in Scheme 1 and 2 with the semiempirical PM6 computational method to further explore their structural features and biological reactivity. We should stress here that while we were working on this paper, a similar experimental part of our work was published. We have decided to present our findings regardless of its agreement or disagreement with the published work [3,7].
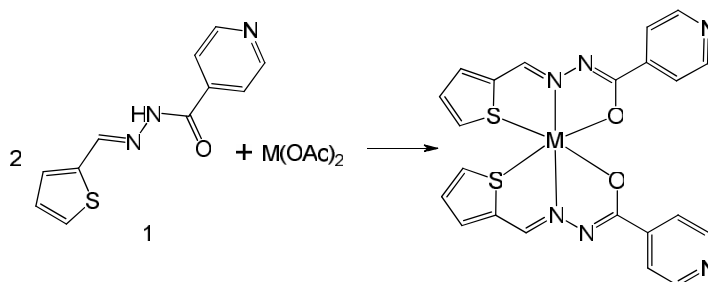
Scheme 1. Metalation of ligand with transition M (II) acetate [TM (II) = Ni (II), Cu (II), Zn (II)]
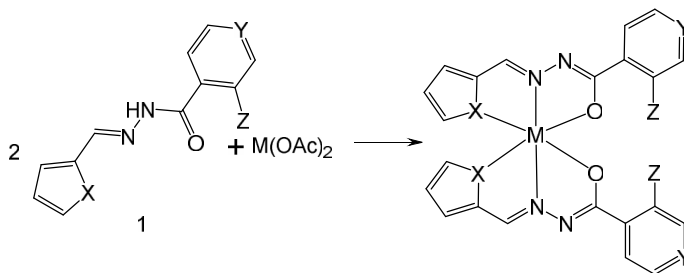
M(II)	Co: (1,5,9,13,17,21), Cu: (2, 6,10,14,18,22), Ni: (3,7,11,15,19,23), Zn: (4,8,12,16,20,24) Mn: (25,26,27,28.29.30)					
Comp.	1 - 4	5 - 8	9 - 12	13 – 16, 25, 28	17 – 20, 26, 29	21 – 24, 27, 30
X	O	S	O	S	O	S
Y	CH	CH	CH	CH	N	N
Z	H	H	OH	OH	H	H

Scheme 2. Studied transition metal (II) complexes with SNO- and ONO- functionalized ligand (1-30)

2. EXPERIMENTAL WORK

Metal(II) complexes were prepared by the reaction of ligand (1) with metal acetate according to Scheme 1 in 2:1 molar ratio respectively.

2.1 Material and Methods

Thiophene-2-carbaldehyde, isonicotinoylhydrazide were obtained from Merck, and all metal (II) acetate salts were purchased from Aldrich and used as received. Commercially available solvents were used as received.

IR spectra were obtained as KBr discs on Perkin-Elmer 237 infrared spectrometer. UV–Vis spectra of DMF solutions of the complexes were recorded on a SHIMADZU UV–Vis spectrophotometer (UV-1601). Conductivity measurements were made on a PHYWE conductivity meter. [1]H-nmr spectra were recorded on a Brucker 300 MHz instrument for solutions in DMSO-D_6 at 21ºC, using TMS as an internal reference. Chemical shifts are expressed in δ(ppm) downfield from TMS. Mass spectra were measured using electroionization technique and melting points (uncorrected) were determined on an electrothermal melting temperature apparatus.

2.2 Ligand Synthesis

2.2.1 Preparation of 2-thiophenecarbaldehyde isonicotinoylhydrazone (1)

The Schiff base ligand (1) used in this work was readily accessible by condensation of Thiophene-2-carbaldehyde with isonicotinoylhydrazide in 1:1 mole ratio in ethanol and few drops of acetic acid were used as a catalyst. The reaction mixture was refluxed for 2 hours. Cooling the solution precipitated the ligand (1) in good yield (86.54%). mp: 125ºC. ESI MS: m/z 232 (M^++1). UV/vis (nm): 323, 268. ^{1}H NMR (d_6-DMSO): δ (ppm): 7.5-8.7 (Pyr-H), 7.3 (s, CH=N), 10.9 (s, NH) 4.5-5.8 (thienyl-H). IR(cm^{-1}): 3243 (NH), 1702 (C=O), 1632 (CH=N), 1020 (N-N).

2.3 Synthesis of the Complexes

The metalation of this ligand with transition metal (II) acetate [TM (II) = Co (II), Cu (II), Ni (II), and Zn (II)] in 2:1 ligand to metal mole ratio yielded six coordinate complexes in which the Schiff base ligands act as S, N, O tridentate ligands forming stable 5-membered rings by binding with the thiophene-S, the imine-N, and the amide-O atoms.

The complexes were prepared by mixing 2.0 mmol of the ligand (1) dissolved in about (30 mL) of methanol, with 1.0 mmol of the metal (II) acetate in (20 mL) hot methanol. The resulting mixture was refluxed for 2 hours and left to stir overnight. The solution was concentrated, then the precipitate was filtered and washed with petroleum ether (40-60ºC). The following complexes were prepared using this method:

*Cis-Bis [*2-thiophenecarbaldehyde isonicotinoylhydrazone*] nickel (II)*

From 0.46 g 2-thiophenecarbaldehyde isonicotinoylhydrazone: Yield: 0.49 g (95%) yellow, mp: 233- 235ºC. ESI MS: m/z 521.0 (M^+). UV/vis (nm): 368.77, 265.00. IR (cm^{-1}): 1632 (CH=N), 1244 (C-O), 1027 (N-N), 455 (Ni-O).

*Cis-Bis [*2-thiophenecarbaldehyde isonicotinoylhydrazone*]copper(II)*

From 0.46 g 2-thiophenecarbaldehyde isonicotinoylhydrazone: Yield 0.37 g (72%) green, mp: 230-232ºC. ESI MS: 524.0 (M^+). UV/vis (nm): 367.27, 263.98. IR (cm^{-1}): 1628 (CH=N), 1242 (C-O), 1025 (N-N), 455 (Cu-O).

*Cis-Bis [*2-thiophenecarbaldehyde isonicotinoylhydrazone*]zinc(II)*

From 0.46 g 2-thiophenecarbaldehyde isonicotinoylhydrazone: yield: 0.50 g (96%) yellow, mp: 227-229ºC. ESI MS: m/z 525.0 (M^+). UV/vis (nm): 368.09, 267.00. ^{1}H NMR (d_6-DMSO):

δ (ppm): 7.7-8.8 (Pyr-H), 7.5 (s, CH=N), 4.6-5.8 (thienyl-H). IR (cm^{-1}): 1627 (CH=N), 1241 (C-O), 1025 (N-N), 455 (Zn-O).

2.4 Conductivity Measurements

The molar conductance of the complexes measured in DMSO solution were found extremely low and almost negligible, which indicates that the complexes are non-conductive and the whole complex is neutral with two uninegative ligands [15].

2.5 IR Spectra

IR spectra of the ligand exhibits a sharp N-H stretching band at 3240-3260 cm^{-1} and an absorption band of 1702 cm^{-1} attributed to C=O stretching. However, these bands are entirely unavailable in the complexes spectra while a new C-O band at 1240-1245 cm^{-1} appears.

2.6 Mass Spectrometry

The mass spectra of each of the complexes shows a peak attributed to a ligand plus proton ion and the molecular ion peak of the complex, which ensures the proposed structure while confirming the loss of one proton by each ligand upon complexation.

2.7 NMR Spectra

Unfortunately, due to paramagnetic electron configuration ^{1}H NMR spectra for the complexes of Ni(II) and Cu(II)were not helpful enough to identify the functional group. For Zn(II) complexes, the spectra successfully elaborates basic information about its complexes, where no peak has been detected for the NH proton while minor changes in the aromatic region along with its chemical shift are noticed. However, the complexity of the signals makes it useless for interpretation. The chemical shift observed for the CH=N proton about 7.5 ppm is an evidence for the contribution of N in coordination to the central Zn(II).

2.8 Electronic Spectra

Absorption spectra were obtained in DMF where a strong band near 369 nm attributed to a charge transfer transition is observed [16].Also, few bands of moderate intensity in the range of 254-268 nm are detected. A band below 268 nm is due to intra-ligand transition, which is the same case for the free ligand.

3. COMPUTATIONAL WORK

The molecular geometries of the investigated TM(II) complexes (1- 24**)** depicted in Scheme2were fully optimized with the semiempirical PM6 method using SPARTAN 10 software, version 1.0.1 without any applied molecular symmetry constraints [12].

The optimized structures were properly attributed to their local minima at the same level of theory with no imaginary frequencies. Then, the density functional theory was employed with 6-31G* basis set to compute various properties including energies of frontier orbitals (ε_H, ε_L), and dipole moment (μ) beside six other QSAR descriptors [17].

The electrostatic potential $V_{(r)}$ created at any point r in the space surrounding a molecule by its nuclei and electrons can be calculated from eq. (1), where Z_A is the charge on nucleus A, at a distance R_A, and $\rho(r)$ is the electronic density. The sign of $V_{(r)}$ at any point r is depends on whether the positive contribution of the nuclei or the negative contribution of the electrons is dominant there. Usually, research is much concerned with the values of V_{min} and V_{max} as a measure of site-specific reactivity of the system [18].

$$V(r) = \sum_A \frac{Z_A}{|R_A - r|} - \int \frac{\rho(r')dr'}{|r' - r|}$$

(1)

Each of the attained wavefunctions was used again at density functional level (B3LYP/6-31G*) to compute six descriptors attributed to the surfaces of electron density (*EDS*) and molecular electrostatic potential (*MEP*). The computed descriptors are the polar area (*PA*), the minimum and maximum values of the electrostatic potential, (V_{min}, V_{max}), the minimum value of the local ionization potential (IP_{min}) as mapped onto an EDS, the the exposed area (A_{ex}) of the transition metal atom in a space-filling model and its electrostatic charge (q_{elec}). The computed descriptors were used to foresee the biological activity of the untested Mn^{+2} complexes.

4. RESULTS AND DISCUSSION

The experimental data and all the antimicrobial activity data related to the synthesized compounds were obtained from the literature for the studied complexes [7]. The antimicrobial activity is expressed as the zone of inhibition (*IZ*) produced by the system. All experimental and computed data of properties and descriptors are listed in Tables 1-3 including, ε_H, ε_L, μ, *PA*, V_{min}, V_{max}, IP_{min}, q_{elec}, and A_{ex}.

4.1 Geometries and Other Properties

A selection of the computationally-optimized geometries of the complexes of Co^{+2}, Cu^{+2}, Ni^{+2}, and Zn^{+2} -as described early- are depicted in Fig. 1 (a-h). Also, central bond lengths and bond angles in the complexes studied are listed in Table 1. Obviously, the complexes are not limited in their shape to octahedron and may convert to other geometries as indicated by the nonzero dipoles listed in Tables 1 and 2.

In Co(II) complexes (1,5,9,13,17,21),, the optimized structures supported by the calculated angles and bond lengths indicate that the coordinated ligands form two five-membered chelate rings upon coordination to the Co(II), Fig. 1(a, b). This, in its turn, imposes large distortions on the ideally octahedral coordination angles. The *trans*-N-Co-N angles are close to 180°, whereas both the *trans*-O-Co-O and the *trans*-S-Co-O angles deviate noticeably from linearity, while the *cis*-O-Co-O and the *cis*-S-Co-O angles show a significant deviation from 90°. The distortion of the coordination sphere around the metal, which has been observed in other similar reported complexes, is a result of the ligand's rigidity [19,20].

For the hexacoordinated Cu (II) complexes (2, 6, 10, 14, 18, 22), Fig. 1 (c, d), the common Jahn–Teller tetragonal distortion takes place impacting the octahedral symmetry [21]. Evidently, the central Cu-N and Cu-O bonds are remarkably long with 2.32 and 2.22 Å respectively when compared to four coordination bonds. Also, when the large S atom is bonded to Cu(II) such as in structures (6, 14, 22), a sharp change in N-Cu-N angles (147.8)

arises compared to the situation when O atoms is available for coordination in the complexes.

For Ni (II) complexes depicted in Fig. 1 (e, f), the computed bond lengths and angles reveal square planar optimized structures (3, 11, 19). The computed bond angles for both the *trans*-N-Ni-N and *trans*-O-Ni-O (close to 180°) and the distance between Ni-O (longer than 3.2 Å) are complement with the common trend in such complexes. Obviously, there is no chemical bonding between Ni and O, where stable square planar complexes of four coordinates are formed. However, when S is available in Ni (II) complexes (7, 15, 23), the calculations predict the formation of distorted octahedral structure.
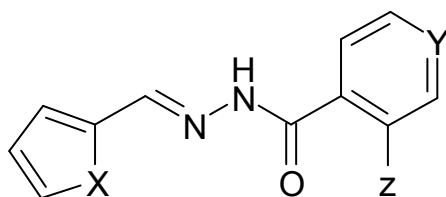
Schiff base	L1	L2	L3	L4	L5	L6
X	O	S	O	S	O	S
Y	CH	CH	CH	CH	N	N
Z	H	H	OH	OH	H	H

Table 1. Computed parameters and antibacterial activity data of the schiff bases

Schiff Base	ε_H eV	ε_L eV	ε_{H-L} eV	μ debye	PA A^2	V_{min} kJ/mol	V_{max} kJ/mol	IP_{min} kJ/mol	Microbial		
									a	b	c
L1	-5.98	-1.14	-4.84	5.65	63.07	-252.89	161.90	35.84	2	2	2
L2	-6.37	-0.85	-5.52	5.32	56.96	-249.86	165.28	36.19	2	1	1
L3	-6.89	-1.30	-5.59	6.89	74.48	-275.37	318.47	34.56	2	1	2
L4	-6.08	-1.14	-4.94	6.43	68.43	-272.47	304.18	35.14	2	2	1
L5	-6.18	-1.29	-4.89	5.20	80.04	-234.11	185.45	34.15	2	1	2
L6	-6.56	-1.18	-5.38	5.00	74.41	-231.80	187.25	34.07	1	2	2
av.	-6.34	-1.15	-5.19	5.75	69.57	-252.75	220.42	34.99			
s	0.34	0.16	0.34	0.75	8.48	18.41	71.30	0.89			

Zn (II) complexes in Fig. 1(g,h) show arrangement with severe angular distortion. The computed bond lengths and angles (4, 12, 20). Evidently, the O-Zn-O, and N—Zn—N and bond angles are (88.3 - 148.7) and (136.2-163.0), respectively. Also, while the computed average Zn-O and Zn-N lengths are closely equal with around 2.00 Å, when S is available in complexes (8, 16, 24), the structure is distorted into trigonal bipyramidal or into distorted square pyramidal based with Zn-S lengths of 3.5 Å, which is a solid evident for a distorted complex structure.

4.2 Antibacterial Properties

The title Schiff bases and their metal(II) chelates were evaluated in reference 7 for their antibacterial activity against the standard bacterial strains of a) *Escherichia coli*, b) *Staphylococcus aureus*, and c) *Pseudomonas aeruginosa*. The compounds were tested at a concentration of 30 *µ*g/0.01 mL in DMF solution. The inhibition zones for *E. coli (a),*

S. aureus (b) and *P. aeruginosa* (c) were measured in mm and the results are listed in Tables 1 and 3 in terms of relative numbers 1, 2, 3 and 4 representing: (27– 45%), (45–64%), (64–82%), and (82–100%) of % inhibition respectively. All the Schiff bases were found to be biologically active and their metal (II) complexes showed significantly enhanced antibacterial activity against one or more bacterial species in comparison to the free Schiff bases. It is however known that chelation such as in (5, 7, 17) tends to make the ligands act as more powerful, thus killing more of the bacteria than the parent Schiff bases do [22]. Frequently, a general reduction of the complex's dipole moment was counted a factor behind increasing the biological activity.
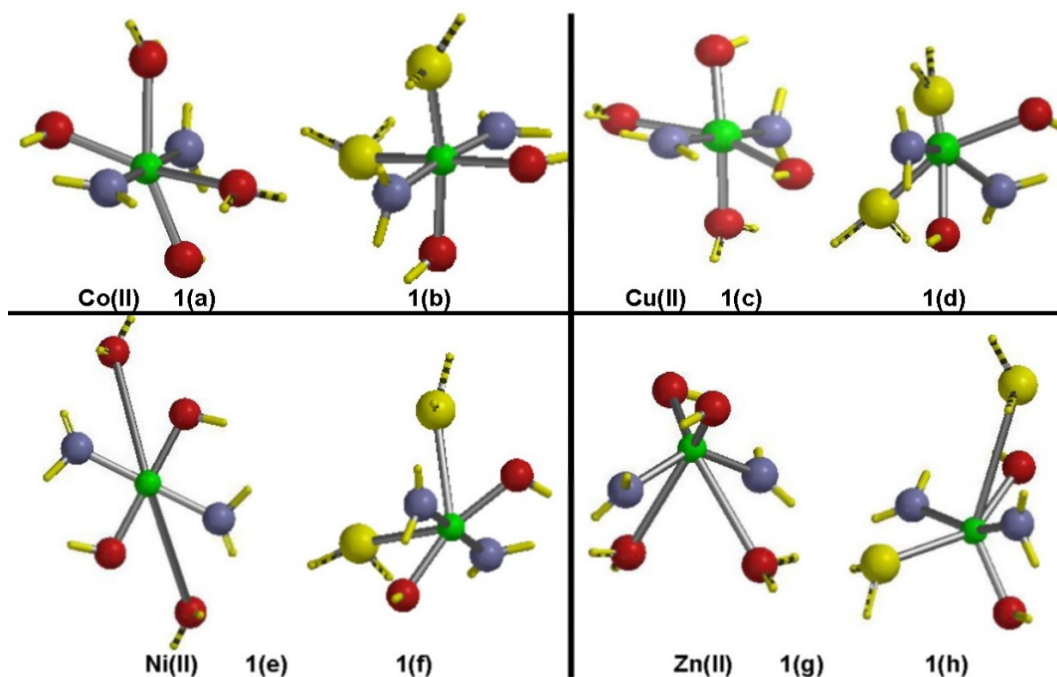

Fig. 1. Optimized M(II) skeleton complexes

4.3 Electrostatic Potential and Electron Density

According to the crystal field theory (CFT), the metal cation is affected by the purely electrostatic field created by the nearest neighbor ligands represented by point charges or point dipoles [23].

Following Bader *et al* in taking the surface to be a particular outer contour of the molecule's electronic density [24], Fig. 2 (a-d)shows examples of electrostatic potentials on $\rho(r) = 0.002$ au molecular surfaces of the ligands and complexes; (1, 7, 14, 21) subsequently. The computed potential's maxima (V_{min}, V_{max}), PA, IP_{min}, q_{elec}, and A_{ex} along with their subsequent averages and standard deviation are listed in Tables 2 - 4.

For each individual Schiff base, a systematic decrease in each of the computed surface related properties was obvious with sulfur (S) atom compared with Oxygen (O) atom. As shown in Table 2, the smallest computed PA for example, is associated with the absence of

lone pairs in S atom (14), while when lone pairs exist with both O and N atoms, PA shows a high increase with 83.33 A^2 (5). However, the average computed values are 67.3 A^2, -328.2 kJ/mole, 196.5 kJ/mol, and 51.3 kJ/mol for *PA, V_{min}, V_{max}, and IP_{min}* respectively.

Though two bidentate ligands are common constituents of each of the complexes studied, a significant variance was concluded in each set of the computed surface related quantities with averages of 105.8 A^2, -324.0kJ/mol, and 52.8 kJ/mol for *PA, V_{min}, and IP_{min}* respectively (Table 3). Obviously, these averages are comparable with their computed counterparts for each of the single ligand indicating the significance of these quantities as a possible function of their biological activity. However, the computed V_{max} for Z(II) complexes Unexpectedly jump to thousands. The $V_{S,min}$ are all within a relatively narrow range, –289.4 to –386.0 kJ/mole, which may infer their primary importance in the structures activity.

4.4 Exploring Manganese (II) Complexes

Manganese (II) complexes are commonly available in active centers of enzymes and various integrins [9-10]. There has been extensive experimental and theoretical research on Mn(II) complexes with various ligands. It has been widely assumed that octahedral Mn(II) complexes are dominantly high-spin molecules [23]. However, researchers frequently tended to question these long term findings. Consequently, low-spin complexes of the metal such as $[Mn(CN)_6]^{4-}$ have been studied because of their occurrence in biological systems. Interestingly, the predicted spin-state of most complexes varied depending on the employed computational method and basis set.

In this part of the work, basic investigation concerning the geometry of Mn(II) complexes are discussed in view of our preceding findings. The Mn(II) complex in the this study is expected to be of a high-spin octahedral. Two optimization calculations using the semiempirical PM6 with spin multiplicity of 2 and 6 concluded that the highest spin multiplicity islowestin energy. Also, a single point calculation using B3LYP/6-31G* could not even proceed with the low spin geometry while ended properly with spin multiplicity of 6.

The computed geometry is summarized in Table 4, while basic structures are depicted in Fig. 3. The computed angles at the Mn(II) center show large deviations from the ideal octahedral values of 90º and 180º, the N-Mn-N and O-Mn-O angles are 128.3º and 91.95º respectively, These angles are close to those in Zn(II) complexes. The bond lenghts in Mn(II) coordination geometry are 2.91 and 1.95 Å for Mn-O and 1.79 Å for Mn-N which are similar to that of Zn(II) complexes.

Table 2. Central bond lengths (Å) and bond angles in the studied complexes

M(II)	Sys	O-M	O-M	O-M-O	S-M	S-M	S-M-O	S-M-O	O-M	O-M	O-M-O	N-M	N-M	N-M-N
Co(II)	1	2.17	2.00	156.3					2.17	2.00	69.2	1.81	1.81	179.4
	5	1.98	1.979		2.13	2.03	76.5	168.8				1.82	1.82	175.13
	9	2.16	2.02	156.3					2.17	2.02	69.2	1.814	1.81	179.2
	13	1.99	1.99		2.13	2.03	76.2	168.6				1.814	1.83	174.9
	17	2.17	2.00	156.4					2.17	2.00	69.4	1.81	1.81	179.4
	21	1.97	1.97		2.12	2.03	86.4	167.5				1.81	1.82	174.2
Cu(II)	2	2.10	2.00	156.3					2..10	2.00	72.9	1.86	1.86	178.0
	6	2.21	2.21		1.21	2.08	87.1	154.0				2.32	2.12	147. 9
	10	2.10	2.03	156.1					2.09	2.03	72.5	1.86	1.85	177.9
	14	2.23	2.23		1.21	2.08	77.6	154.1				2.32	2.11	148.0
	18	2.10	2.00	156.3					2.10	2.00	72.8	1.86	1.86	178.4
	22	2.21	2.21		1.21	2.07	76.6	153.9				2.33	2.11	147.3
Ni(II)	3	1.86	1.86	180.0					3.21	3.21	111.9	1.86	1.86	179.4
	7	1.89	1.89		2.67	2.67	60.2	137.3				1.87	1.87	174.4
	11	1.88	1.88	180.0					3.41	3.65	114.5	1.87	1.87	177.9
	15	2.34	2.34		2.16	2.41	63.7	163.6				1.86	1.86	176.2
	19	1.87	1.87	180.0					3.80	3.83	114.4	1.87	1.87	180.0
	23	1.89	1.90		2.68	2.68	59.9	137.3				1.87	1.87	174.4
Zn(II)	4	2.00	2.00	148.5					2.99	2.99	88.3	1.95	1.95	136.2
	8	2.08	2.08		3.48	2.43	46.4	142.6				2.02	2.09	161.4
	12	2.00	2.00	148.7					2.98	2.99	88.5	1.94	1.95	137.1
	16	2.06	2.06		3.51	2.47	48.3	148.3				2.02	2.07	154.4
	20	2.00	2.00	148.6					3.00	2.99	88.5	1.95	1.95	136.8
	24	2.08	2.08		3.50	2.42	45.8	141.8				2.03	2.10	163.0

Table 3. Computed parameters and antibacterial activity data of the metal(II) complexes

| M(II)	Sys	ε_H eV	ε_L eV	ε_{H-L} eV	μ debye	PA A^2	V_{min} kJ/mol	V_{max} kJ/mol	IP_{min} kJ/mol	q_{elec}	A_{ex}	Microbial		
												a	b	c
Co(II)	1	-5.15	-1.79	-3.36	3.67	126.99	-184.13	111.51	33.36	0.70	1.82	3	2	3
	5	-4.68	-2.05	-2.63	3.62	127.11	-195.92	112.07	33.79	0.69	0.11	4	3	3
	9	-5.12	-1.79	-3.33	5.22	149.98	-244.00	257.55	33.32	0.73	1.81	3	3	2
	13	-4.76	-2.11	-2.65	4.21	163.49	-233.80	251.77	32.99	0.67	0.12	2	2	3
	17	-5.50	-2.17	-3.33	6.97	127.43	-199.64	133.66	32.82	0.73	1.79	4	3	2
	21	-4.91	-2.37	-2.54	6.45	127.39	-200.40	134.64	32.79	0.90	0.14	3	4	3
	av.	-5.02	-2.05	-2.97	5.02	137.07	-209.65	166.87	33.18	0.74	0.96			
	s	0.30	0.23	0.40	1.44	15.82	23.62	68.76	0.39	0.08	0.92			
Cu(II)	2	-5.10	-1.87	-3.23	3.87	125.39	-183.71	113.35	33.35	0.47	2.53	3	3	2
	6	-4.92	-2.04	-2.88	2.65	98.41	-172.74	114.46	33.74	0.41	1.45	3	3	2
	10	-5.07	-1.88	-3.19	5.28	148.69	-245.82	256.24	33.49	0.40	2.54	3	3	3
	14	-4.89	-2.04	-2.85	5.25	132.86	-220.62	266.67	33.78	0.25	1.42	3	3	3
	18	-5.47	-2.25	-3.22	7.45	128..21	-200.43	134.09	32.78	0.54	2.54	3	3	2
	22	-5.27	-2.47	-2.80	5.95	108.69	-203.13	138.04	32.64	0.44	1.62	3	3	3
	av.	-5.12	-2.09	-3.03	5.08	122.81	-204.41	170.48	33.30	0.42	2.02			
	s	0.22	0.23	0.20	1.66	19.83	26.18	71.25	0.48	0.10	0.57			
Ni(II)	3	-5.30	-1.91	-3.39	1.19	104.81	-162.51	107.31	28.39	0.70	4.69	3	2	4
	7	-5.18	-1.95	-3.23	1.24	79.21	-157.27	108.10	32.53	0.69	2.77	4	2	3
	11	-5.40	-1.95	-3.45	3.75	124.53	-194.36	269.64	29.01	0.69	4.86	3	3	3
	15	-4.96	-2.37	-2.59	5.71	152.72	-226.06	262.21	33.36	0.50	1.49	3	4	2
	19	-5.72	-2.25	-3.47	7.10	127.79	-202.91	178.61	32.65	1.08	5.52	3	3	3
	23	-5.65	-2.32	-3.33	8.00	128.78	-202.88	140.55	32.67	0.83	0.70	4	3	2
	av.	-5.37	-2.13	-3.24	4.50	119.64	-191.00	177.74	31.44	0.75	3.34			
	s	0.29	0.21	0.33	2.92	24.99	26.35	73.18	2.15	0.19	1.98			
Zn(II)	4	-5.37	-1.93	-3.44	4.20	122.88	-175.92	114.50	33.92	1.17	5.68	3	2	3
	8	-5.45	-2.07	-3.38	3.62	102.70	-171.64	128.21	33.54	1.09	4.35	2	3	4
	12	-5.25	-1.93	-3.32	5.00	142.59	-239.00	250.94	33.61	1.16	5.68	3	4	2
	16	-5.48	-2.08	-3.40	5.84	133.80	-202.79	283.88	32.77	1.09	4.36	2	3	3
	20	-5.74	-2.30	-3.44	7.37	124.43	-200.15	133.62	32.76	1.17	5.73	2	3	2
	24	-5.83	-2.43	-3.40	7.10	113.49	-201.77	150.01	32.67	1.08	4.37	3	3	3
	av.	-5.52	-2.12	-3.40	5.52	123.32	-198.55	176.86	33.21	1.13	5.03			
	s	0.22	0.20	0.04	1.53	14.17	24.10	71.82	0.54	0.05	0.73			
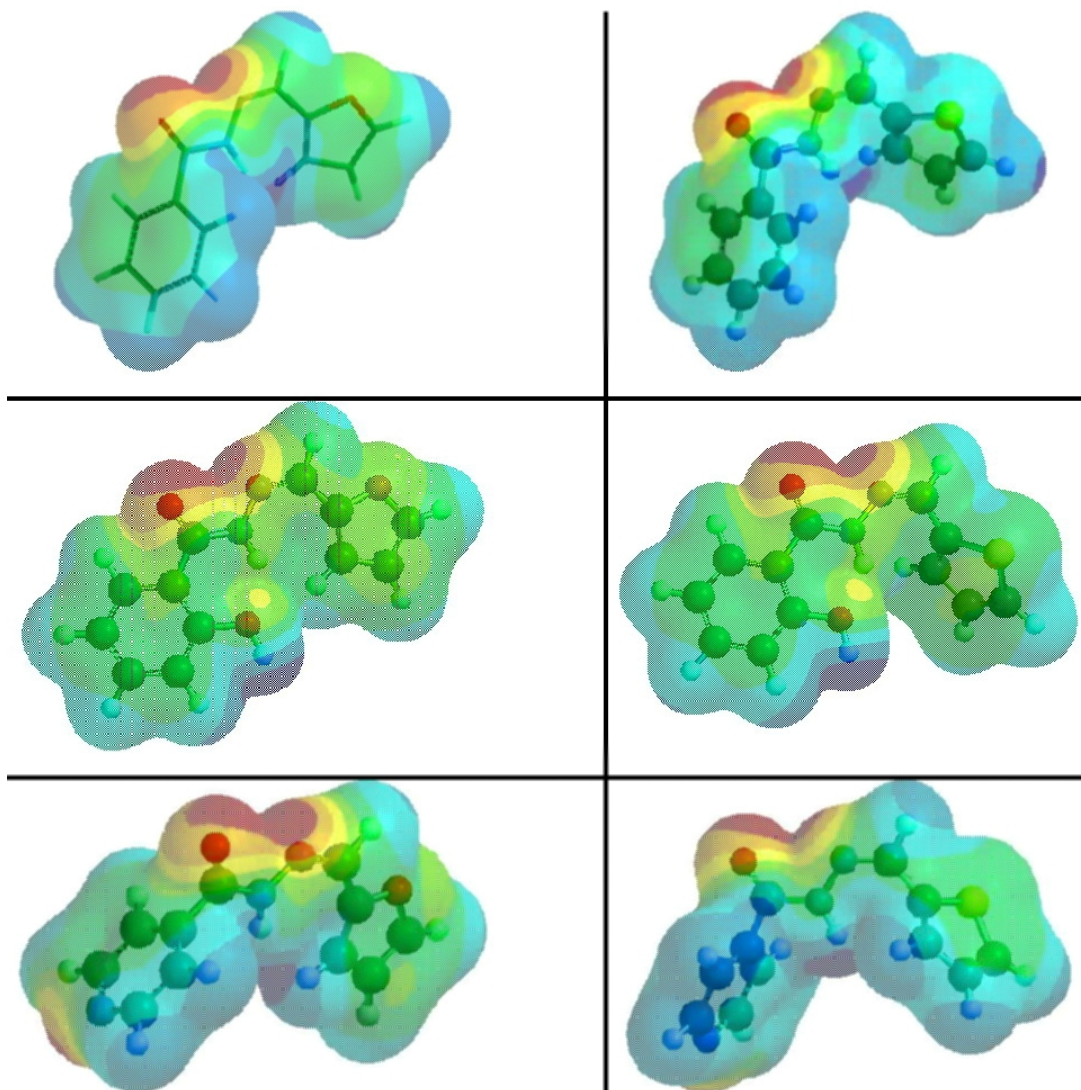
Fig. 2. Computed electrostatic potential on the molecular surface of complexes (1,7,14,21) optimized at PM6. The potential ranges according to the color code: red (most negative) < orange <yellow < green < blue (most positive)

Table 4. Central bond lengths (A) and bond angles in studied Mn(II) complexes

Mn(II)	Mn-O	Mn-O	Mn-S	Mn-N	N-Mn_N	O-Mn-O	S-Mn-S
25	2.83	1.95	-	1.79	130.9	94.7	-
26	3.28	3.28	2.29	1.86	171.5		104.3
27	1.98	3.06	-	1.86	167.7	88.9	-
28	2.03	2.03	2.26	1.87	176.6	93.0	105.0
29	1.95	2.91	-	1.79	178.0	93.6	-
30	2.02	2.02	2.26	1.87	178.7	92.0	111.8
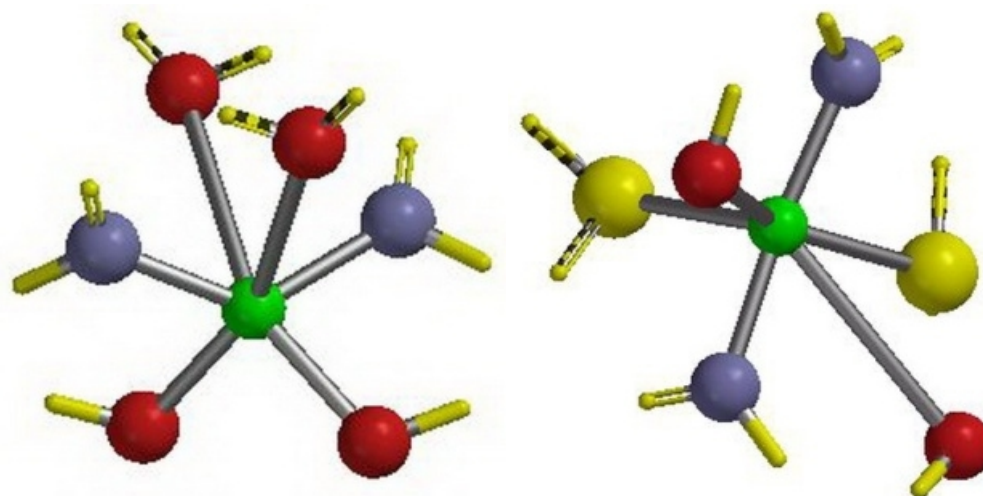
Fig. 3. Optimized Mn(II) skeleton complexes

Thecomputed descriptors including, ε_H, ε_L, μ, PA, V_{min}, V_{max}, IP_{min}, q_{elec}, and A_{ex} for the studied Mn(II) complexes are listed in Table 5. Comparing the averages of the computed values for most of the descriptors with their counterparts for the former complexes in Table 3, one can expect that Mn(II) complexes would have antimicrobial potency ranges between Zn(II) and Ni(II) complexes.

Table 5. Computed parameters of biologically untested Mn(II) complexes

M(II)	Sys	ε_H eV	ε_L eV	ε_{H-L} eV	μ debye	PA A^2	V_{min} kJ/mol	V_{max} kJ/mol	IP_{min} kJ/mol	q_{elec}	A_{ex}
Mn(II)	25	-4.47	-2.05	-2.42	5.45	126.69	-216.34	119.86	33.95	1.19	4.94
	26	-3.65	-2.21	-1.44	5.15	124.36	-172.89	139.73	33.62	0.99	2.28
	27	-3.68	-2.10	-1.58	4.43	123.72	-222.42	256.68	33.83	1.28	5.66
	28	-3.69	-2.15	-1.54	4.71	169.47	-239.92	249.68	32.55	0.89	0.30
	29	-4.71	-2.47	-2.24	9.42	128.82	-201.95	140.67	32.73	1.19	5.16
	30	-4.00	-2.43	-1.57	9.96	138.84	-206.06	141.46	32.57	0.66	0.40
	avg	-4.03	-2.24	-1.80	6.43	135.32	-209.93	174.68	33.21	1.03	3.12
	s	0.46	0.18	0.42	2.57	17.61	22.57	61.38	0.66	0.23	2.45

5. CONCLUSION

The structure of previously synthesized Schiff base ligand coordinated with the Co(II), Cu(II), Ni(II), and Zn(II) metal ions through N, O, and/or S toms have been computationally investigated by PM6 and DFT/6-31G methods. Ten different electronic and surface related quantities were calculated to confirm the geometry of the complexes and to explore their antimicrobial potency. A small standard deviation in most of the calculated mathematical averages for the computed quantities supports the closeness of the experimental potency. Similar Calculations for Mn(II) complexes showed that Mn(II) would thermodynamically prefer a high-spin octahedral with a spin multiplicity of 6. In terms of its antimicrobial activity, Mn(II) complexes would come next to Zn(II) complexes. PM6 semiempirical method can be successfully employed to investigate similarity in molecular features and to predict their individual biological behavior.

COMPETING INTERESTS

Authors have declared that no competing interests exist.

REFERENCES

1. McCleverty JA, Meyer TJ. Comprehensive Coordination Chemistry II, Molina HR, Mederos A, Eds. Elsevier: London. The United Kingdom. 2004;31.
2. Patil SA, Naika VH, Kulkarnia AD, Badami PS. DNA cleavage, antimicrobial, spectroscopic and fluorescence studies of Co(II), Ni(II) and Cu(II) complexes with SNO donor coumarin Schiff bases. Spectrochim Acta A. 2010;75:347.
3. Saadeh SM. Synthesis, characterization and biological properties of Co(II), Ni(II), Cu(II) and Zn(II) complexes with an SNO functionalized ligand. Arabian J Chem. 2013;6:191.
4. Sheng X, Guo X, Lu XM, Lu GY, Shao Y, Liu F, Xu Q. DNA binding, cleavage, and cytotoxic activity of the preorganized dinuclear zinc(II) complex of triazacyclononane derivatives. Bioconjugate Chem. 2008;19:490.
5. Hoge CW, Gambel JM, Srijan A, Pitarangsi C, Echeverria P. Trends in antibiotic resistance among diarrheal pathogens isolated in Thailand over 15 years. Clin Infect Dis. 1998;26:341.
6. Alanis AJ. Resistance to antibiotics: Are we in the post-antibiotic era? Arch Med Res. 2005;36:697–705.
7. Chohan ZH. Synthesis, characterization and biological properties of bivalent transition metal complexes of Co(II), Cu(II), Ni(II) and Zn(II) with some acylhydrazine derived furanyl and thienyl ONO and SNO donor schiff base ligands. Syn React Inorg Met. 2001;31(1):1-16.
8. Luciana S, Francisco JBMJ, Diogo RMM, Marcelo SDS, Ivan RP, Marcus TS. SAR, QSAR and docking of anticancer flavonoids and variants, a review. Curr Top Med Chem. 2012;12(24):2785-2809(25).
9. Singh N, Chaudhury S, Liu R, Abdul Hameed MDM, Tawa G, Wallqvist A. QSAR classification model for antibacterial compounds and its use in virtual screening. J Chem Inf Model. 2012;52:2559−2569.
10. Aptula AO, Kühne R, Ebert RU, Cronin MTD, Netzeva TI, Schüürmann G. Modeling discrimination between antibacterial and non- antibacterial activity based on 3D molecular descriptors. QSAR Comb Sci. 2003;22:113−128.
11. Toropova AP, Toropov AA, Benfenati E, Gini G. Co-evolutions of correlations for QSAR of toxicity of organometallic and inorganic substances: An unexpected good prediction based on a model that seems untrustworthy. Chemometr Intell Lab. 2011;105:215–219.
12. SPARTAN'10 for Windows. Wavefunction, Irvine, Ca; 2010.
13. Hehre WJ, Huang WW, Klunzinger PE, Deppmeier BJ, Driessen AJ. Spartan manual. Wavefunction, Inc. 18401 Von Karman Ave., Suite 370, Irvine, CA 92612; 1997.
14. Stewart JJP. Application of the PM6 method to modeling the solid state. J Mol Model. 2008;14(6):499–535.
15. Geary WJ. The use of conductivity measurements in organic solvents for the characterisation of coordination compounds. Coordin Chem Rev. 1971;7:81-122.
16. Rassolov VA, Pople JA, Ratner MA, Windus TL. 6-31G* basis set for atoms K through Zn. J Chem Phys. 1998;9(4):1223-1229.

17. Dey M, Rao CP, Saarenketo PK, Rissanen K. Mono-, di- and tri-nuclear Ni(II) complexes of N-, O- donor ligands: structural diversity and reactivity. Inorg Chem Commun. 2002;5:924-928.
18. Murray JS, Abu-Awwad FM, Politzer P, Wilson LC, Troupin AS, Wall RE. Molecular surface electrostatic potentials of anticonvulsant drugs. Int J Quantum Chem. 1998;70(6):1137-1144.
19. Yoon JJ, Lee U, Koo BK. Synthesis and crystal structures of Mn(II), Co(II), Ni(II), Cu(II), and Zn(II) metal complexes with NNO functionalized ligands, Bull. Korean Chem Soc. 2005;26:925.
20. Cotton FA, Wilkinson G, Murillo CA, Bochmann M. Advanced Inorganic Chemistry, 6th ed. John Wiley & Sons, Inc. 1999;865.
21. Pal SN, Pushparaju J, Sangeetha NR, Pal S. Copper(II) complexes containing a CuN_4O_2 coordination sphere assembled *via* pyridine-imine-amide coordination: Synthesis, structure and properties. Transit Metal Chem. 2000;25:528−532.
22. Mittal P, Uma V. Coordination behaviour and biological activity of unsymmetrical bis–hydrazone towards manganese (II) Ion. Int J Chem Sci. 2008;6(2):1050-1060.
23. Trzaskowski B, Les A, Adamowicz L. Modelling of octahedral Mn II complexes with inorganic ligands: a problem with spin-states. Int J Mol Sci. 2003;4:503-511.
24. Bader RFW, Carroll MT, Cheeseman JR, Chang C. Properties of atoms in molecules: Atomic volumes. J Am Chem Soc. 1987;109:7968-7979.

Peer-review history:
The peer review history for this paper can be accessed here:
http://www.sciencedomain.org/review-history.php?iid=528&id=16&aid=4700